Supplementary data

Material and methods:

RNA isolation and Real Time PCR: Whole retinas were collected from individual $T17M^{+/-}$ $Rho^{+/-}$ mice at P15. RNA was extracted and cDNAs was prepared as described previously. Real-Time PCR was performed using a custom Taqman array plate with 32 genes including *Gapdh* as endogenous control (Applied Biosystems, Carlsbad, CA). A student's *t* test was performed to compare the levels of relative gene expression in $T17M^{+/-}$ $Rho^{+/-}$ and wild-type sibling at P15 (GraphPad Prism). The fold changes were calculated by dividing the mean of the relative quantities (RQ's) for the $T17M^{+/-}$ $Rho^{+/-}$ mice by the mean RQ of the C57BL/6 mice.

Expression vector and Histology: A full length coding region of human T17M mutant *Rho* and human wild type *Rho* was cloned into AAV(2) vector in frame with eGFP to produce adeno-associated viruses with serotype 5. The human genomic rhodopsin-GFP fusion plasmid was made by eliminating the stop codon from the end of the rhodopsin gene and allowing continuous "in frame" reading through GFP. Expression of the Rho-GFP gene was driven by the proximal mouse opsin promoter.

Both eyes were injected with 1 ul of viral preps (2.5×10^{12} viral genome per ml). Right eyes of P5 C57BL/6 mice were injected with AAV5-hT17M Rho-GFP, left eye received AAV5-hRho-GFP injections. 3 weeks after injections, the mice were sacrificed and RNA was isolated from whole retinas. Taqman Gene Expression assay (Applied Biosystems, Carlsbad, CA) was used to perform RT PCR. We checked differential gene expression of *Eif2α, Bip, ATF4, ATF6, CHOP, Xbp1* and human *Rho* was used as internal control. Eyes from injected animals were inoculated and fixed as described previously. GFP expression was detected using direct fluorescence in 12 µm cryostat retina sections.

Results and Discussion

hT17M *Rho* causes UPR activation in AAV5 injected C57BL/6 retinas.

We injected the C57BL/6 retinas with AAV5-hRho-GFP and AAV5-hT17M Rho-GFP to compare the up-regulation in the UPR-associated gene expression and found significant elevation in expression levels of ATF4,

ATF6, Bip, CHOP and Xbp1 in the mutant injected eyes (by 3.24, 2.73, 2.93, 3.40 and 2.79-fold respectively, $P < 0.05$, Fig.S1, Table S4). To minimize transduction variations of viral delivery the h*Rho* mRNA was used as a normalizer. Results of experiments demonstrated that the over-expression of mutant Rho leads to significant up-regulation of UPR-induced genes (Fig. S1, Table S4).

Consistent with our experiment conducted in T17M $^{+/-}$ Rho $^{+/+}$ ERAI $^{+/-}$ mice (Fig. 1) we also observed mislocalization of mutant hT17M Rho protein compared to wild type Rh. We detected its accumulation in the Outer Nuclear Layer (ONL) and Inner Segments (IS) of photoreceptors (Fig. S1).

ER stress was activated in T17M$^{+/-}$ Rho$^{+/-}$ transgenic mice

In T17M$^{+/-}$ Rho$^{+/-}$ retinas we observed elevation of UPR gene expression at P15 (Figure S2, table S3). The UPR markers like Eif2α, Bip, ATF4, ATF6, Xbp1 and CHOP show significant upregulation (Fold increase ~1.2, ~1.2, ~1.2, ~1.6, ~1.2 and ~ 1.5 respectively; Table S3). These animals may have a faster progressive form of adRP since at P15 we already observed upregulation of apoptotic genes like *Caspase3* (Fold increase ~ 1.5; $P < 0.05$) and pro apoptotic members of Bcl2 family genes like *Bad* (Fold increase ~ 3), *Bax* (Fold increase ~ 1.4), *Bim* (Fold increase ~ 1.4) and *Bid* (Fold increase ~ 1.6). Interestingly, we also observed significant elevation in gene expression of pro-survival genes such as *Bcl2* (Fold increase ~1.4) and chaperons *Canx* (~ 2 Fold increase) and *Hsp90b1* (~1.6 fold increase) as well as genes involved in ERAD like *Syvn1* (~ 1.2 fold increase) (for details please see Fig. S1 and table S3). Other survival pathways like Akt pathway genes do not show any significant difference. It seems that most of the ER stress pathways have been upregulatedat at P15, however, lack of significant difference in expression levels of the *Crx* and *Nrl* genes indicates that cell death has not occurred at this time.

The T17M$^{+/-}$Rho$^{+/-}$ model does not have an extra copy of rhodopsin and shows upregulation of UPR-associated gene expression. Therefore, we can conclude that the T17M Rho mutation itself and not overdose of *Rho,* causes ER stress response.

Autophagy genes were induced in hT17M *Rho* retinas

In hT17M *Rho* retinas, we detected expression of the autophagy-associated genes *Atg5* and *Atg7* as early as at P15 (~1.3 fold increases, $P < 0.01$ and $P < 0.05$, respectively) (Fig. S3, Table S1). Moreover, the expression of both genes was elevated at all subsequent time points, although significant differences were observed only at P18 and P25.

Akt pathway gene were induced in hT17M *Rho* retinas

We measured the expression of *Akt1* and *Akt2*, which are involved in cell survival pathways (Fig. S4, Table S1). At P21, we observed activation of both *Akt1* (~1.3 fold increase, $P < 0.05$) and *Akt2* (~1.4 fold increase, $P < 0.05$). *Akt1* continued to be up-regulated at P25 (~1.5 fold increase, $P < 0.0001$), while *Akt2* showed no change compared with the control (Fig. 4). Interestingly, *pTen*, which is involved in post-transcriptional modification of Akt, was also overexpressed at P21 and P25 (~1.3 and ~1.9 fold increase, $P < 0.05$ and $P < 0.0001$, respectively).

Supplementary Figure Legends:

Figure S1. A: Direct microscopy images of C57Bl6 retinas injected with AAV5-hRho-GFP and AAV5-hT17M Rho-GFP. A, B, C – retinas over-expressing the wild-type Rho, D,E,F – retinas over-expressing the mutant. Scale bar indicates 20 µm (A and D) and 45 µm (B,C,E,F). We observed Rho mislocalization in IS and ONL (D, E, F) in retinas injected with mutant Rho while over-expressed wild-type Rho traffics to OS of photoreceptors (A, B, C). B: Over-expression of mutant hT17M *Rho* in photoreceptors leads to elevated UPR-gene expression compared to over-expressed wild-type *Rho*. Please see details in Table S4.

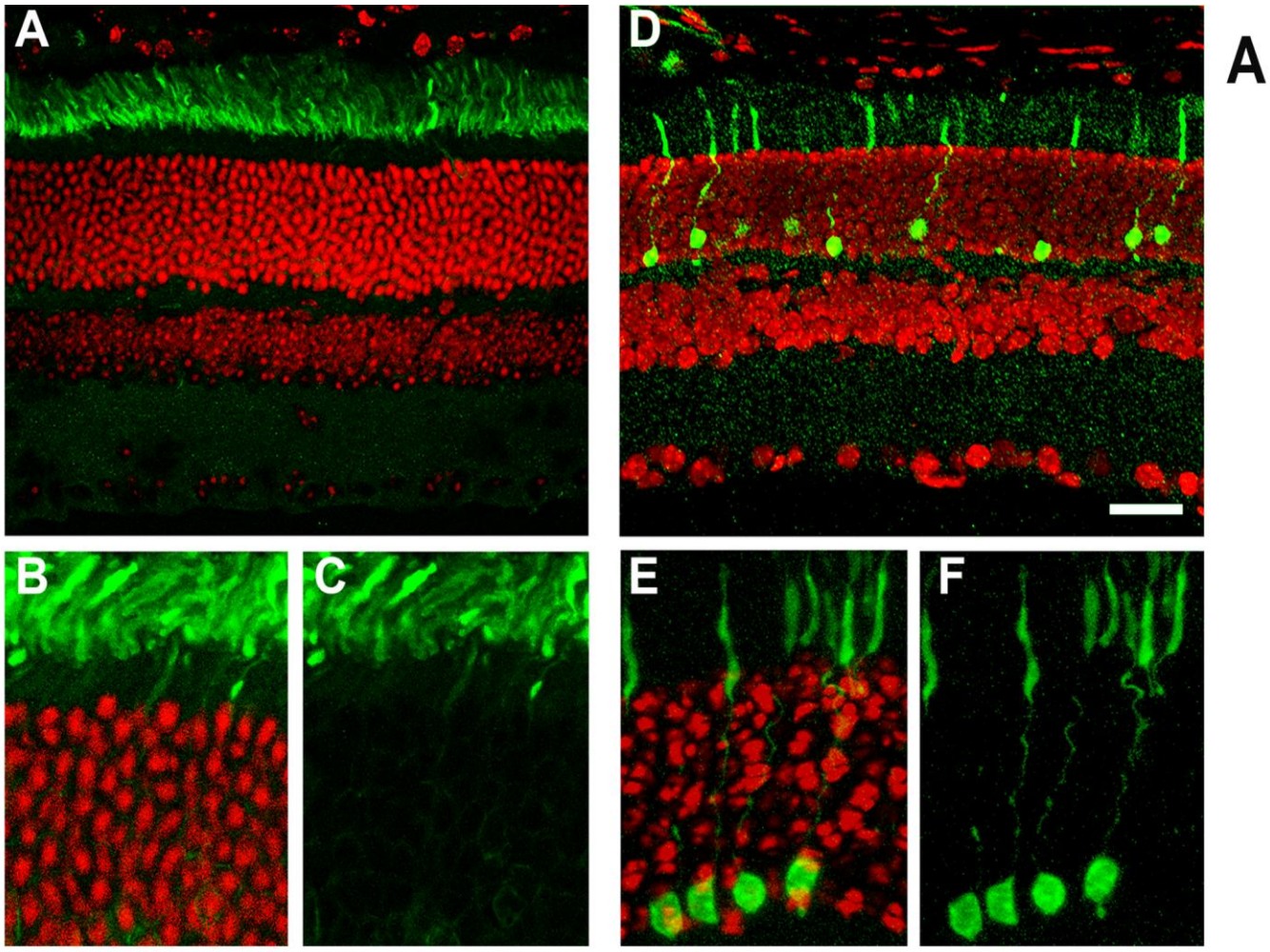
A
D
A
B
C
E
F

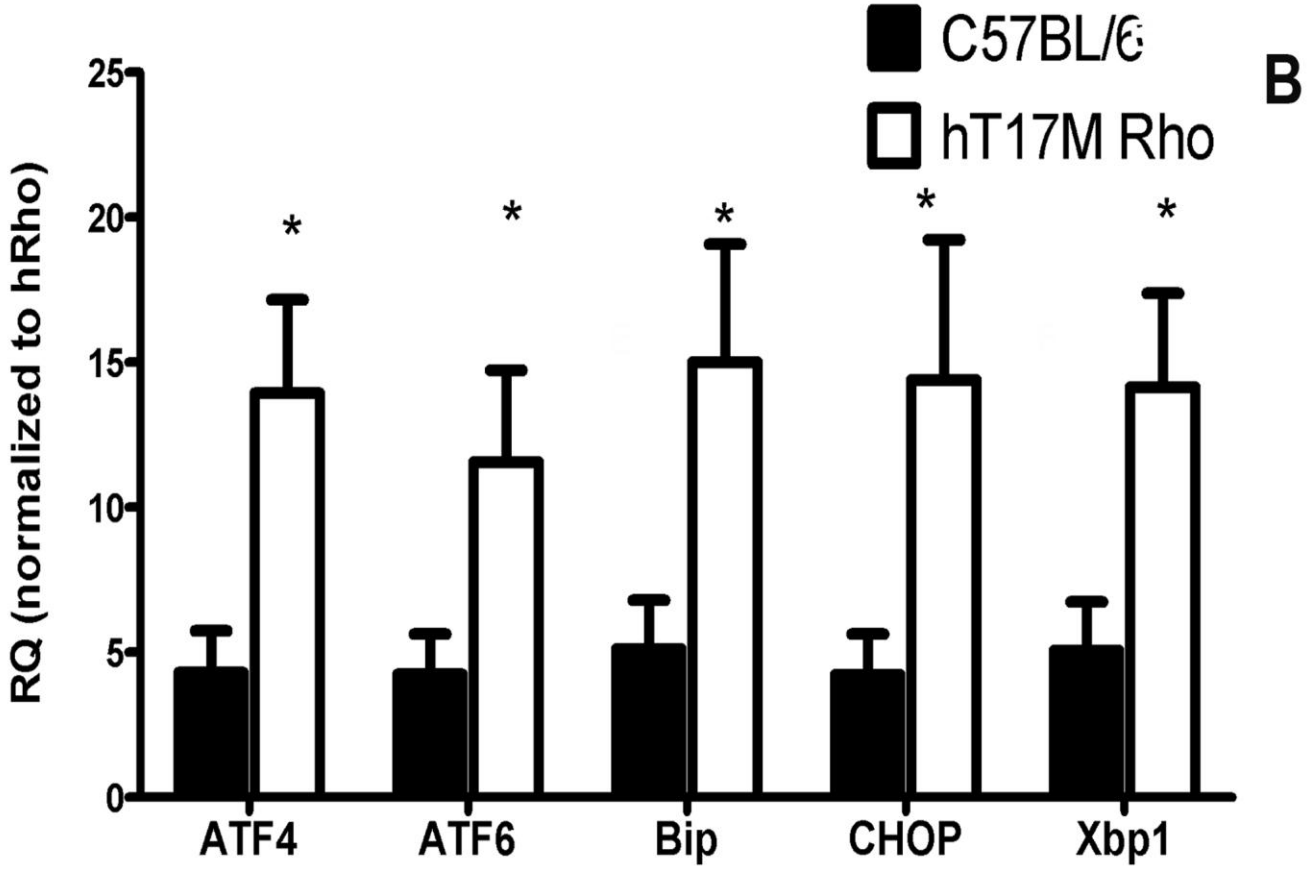
C57BL/6
hT17M Rho
B
RQ (normalized to hRho)
25
20
15
10
5
0
*
*
*
*
*
ATF4
ATF6
Bip
CHOP
Xbp1

Fugure S2. UPR-associated genes are up-regulated at P15 in hT17M$^{+/-}$ Rho$^{+/-}$ retinas. Wild-type gene expression is normalized to 1, and the ratio of mean RQs of hT17M$^{+/-}$ Rho$^{+/-}$ to that of the wild-type is shown. Please see details in Table S3. (* $p < 0.05$; ** $p < 0.01$; *** $p < 0.001$; **** $p < 0.0001$).

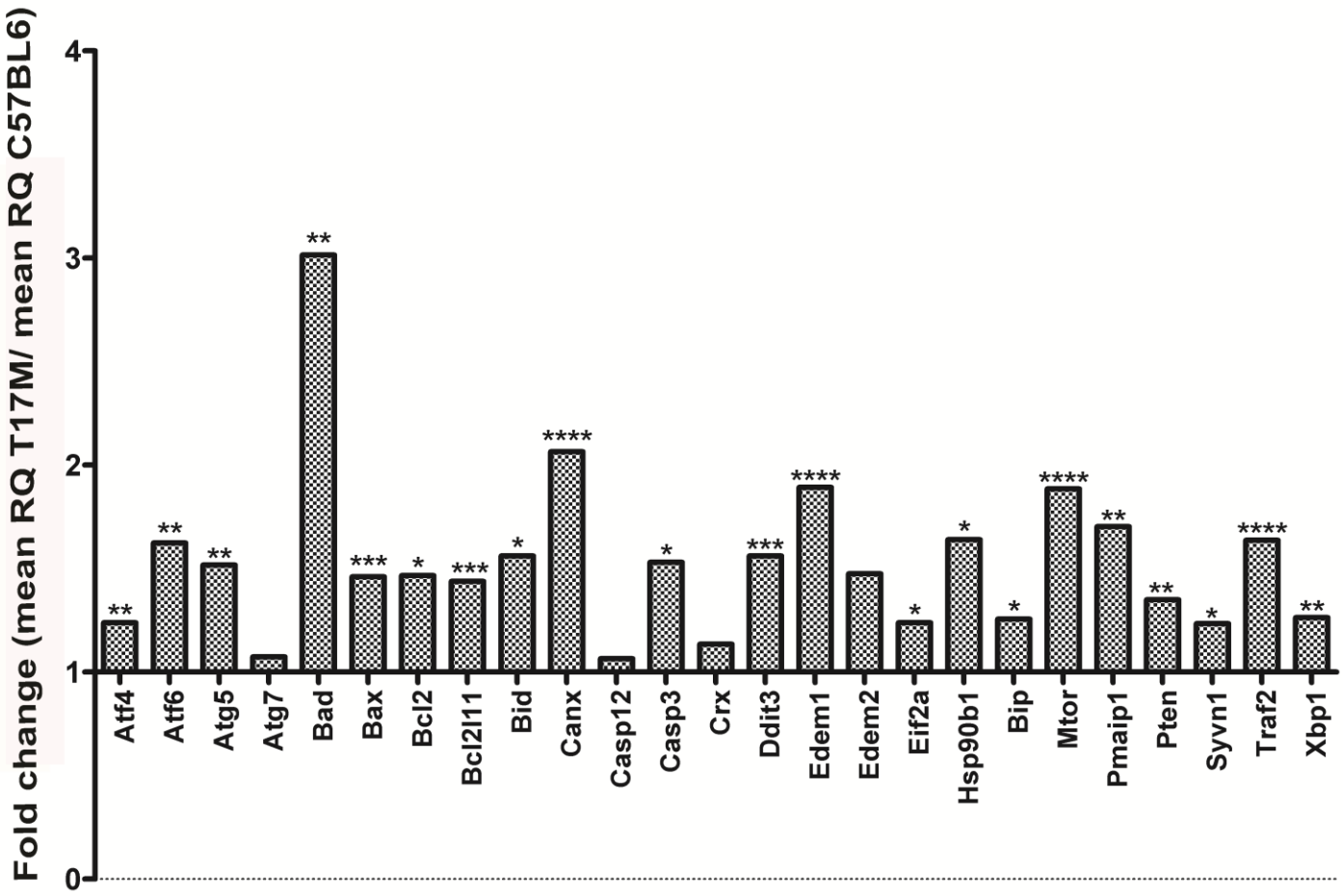

Figure S3. Autophagy genes are steadily elevated in hT17M *Rho* retinas starting at P15. Wild-type gene expression is normalized to 1, and the ratio of hT17M *Rho* to the wild type is shown. *Atg5* gene expression is increased (1.3-fold increase, P < 0.01). *Atg7* gene expression is amplified 1.3-fold (n = 4) (* $p < 0.05$; ** $p < 0.01$; *** $p < 0.001$; **** $p < 0.0001$).

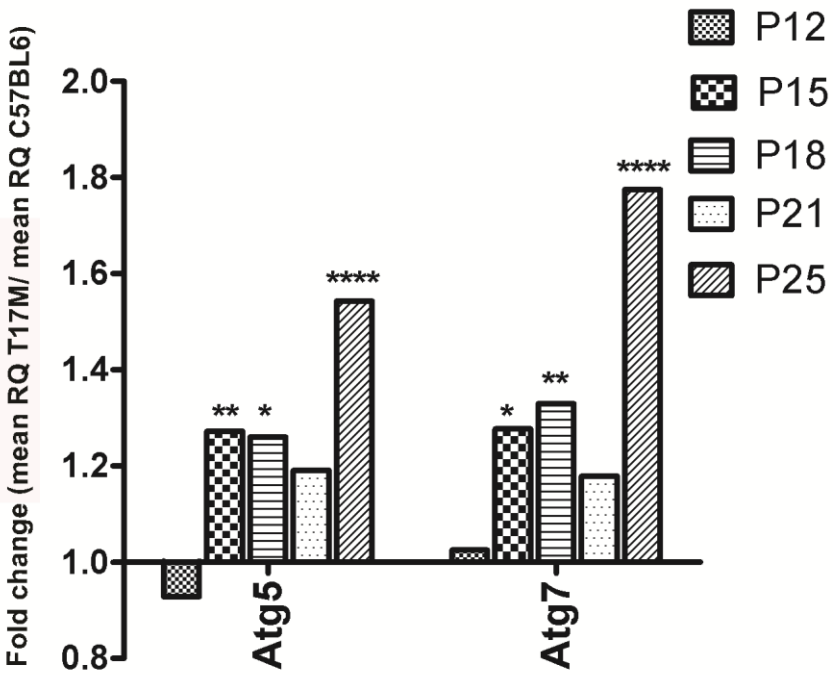

Figure S4.Genes involved in the AKT survival pathway are up-regulated at P21 in hT17M *Rho* mice. Wild-type gene expression is normalized to 1, and the ratio of hT17M *Rho* to the wild type is shown. *Akt1* gene expression is increased by 1.3- and 1.5-fold at P21 and P25, respectively. *Akt2* expression is increased by 1.3-fold at P21. *pTen* gene expression is increased by 1.32-fold at P21 and by 1.9-fold at P25. (* $p < 0.05$; ** $p < 0.01$; *** $p < 0.001$; **** $p < 0.0001$)